

August 2020

---

Independent Study (NSCI 202):  
Laboratory Scale Study of Nitrate and  
Arsenic Removal via Permeable Reactive  
Barrier under Cold Conditions



**Yukon  
University**

**Project team:**

Chelsey Zurkan

Student, Yukon University

Dr. Guillaume Nielsen

NSERC Industrial Research Chair in Northern Mine  
Remediation, Yukon University Research Centre

Ben McGrath

Laboratory Technician, Yukon University

This publication may be obtained online at [yukonu.ca/research](http://yukonu.ca/research)

**This publication may be obtained from:**

YukonU Research Centre, Yukon University  
520 University Drive  
P.O. Box 2799,  
Whitehorse, Yukon  
Y1A 5K4  
(867) 668-8895  
1-800-661-0504  
[yukonu.ca/research](http://yukonu.ca/research)

# Table of Contents

List of Abbreviations .....	4
1. Introduction.....	1
2. Materials and Methods.....	3
2.1. <i>Synthetic Mine Water Preparation</i> .....	3
2.2. <i>Column Construction</i> .....	5
2.3 <i>Column Substrates</i> .....	6
2.4. <i>Hydraulic Residence Time</i> .....	7
2.5. <i>Experimental Design</i> .....	7
3. Results and Discussion.....	8
3.1. <i>Porosity and flow rate calculation</i> .....	8
3.2. <i>Arsenic</i> .....	8
3.2. <i>Nitrate</i> .....	12
3.3. <i>pH</i> .....	15
4. Conclusions.....	15
Appendix A .....	22
Appendix B .....	24

## List of Abbreviations

<b>AMD</b>	Acid Mine Drainage
<b>As</b>	Arsenic
<b>DIW</b>	Deionized Water
<b>EC</b>	Electrical Conductivity
<b>Fe</b>	Iron
<b>HRT</b>	Hydraulic retention time
<b>ML</b>	Metal Leaching
<b>NO<sub>3</sub><sup>-</sup></b>	Nitrate
<b>ORP</b>	Oxidation Reduction Potential
<b>PRB</b>	Permeable Reactive Barrier
<b>S</b>	Sulfur
<b>SMW</b>	Synthetic Mine Water
<b>SO<sub>4</sub><sup>2-</sup></b>	Sulfate
<b>TOC</b>	Total Organic Carbon
<b>ZVI</b>	Zero-valent Iron

## 1. Introduction

The mine life cycle, from exploration to mine closure can be fast-paced and volatile, therefore careful consideration should be given to remediation planning of mine sites. Ensuring strategies are developed which are both cost effective, and appropriate to the climate and biome of which the mine site is located, are essential. Of particular concern to gold-mining operations in Northern climates are waste by-products of cyanide degradation; metal leaching (ML) and acid mine drainage (AMD); and extreme cold conditions which have potential to hamper biological processes involved in bioremediation methods.

Exposure of mine tailings to water and oxygen cause acid-generating reactions to occur and the now-reactive tailings become a source of the effluent commonly known as AMD in ground and surface water (Johnson 2003). Generally, AMD is characterized by low pH and high concentrations of sulphate, iron, and dissolved metals (Blowes et al. 1994).

Due to the acidic conditions created by AMD, arsenic sulfidic ore such as arsenopyrite ( $\text{FeAsS}$ ) leaches arsenic from gold heap leaches (Roussel et al. 2000). Arsenic (As) in aquatic environments usually exists in inorganic forms as arsenate ( $\text{As(V)}$ ) and arsenite ( $\text{As(III)}$ ). As (III) is usually more mobile and toxic than As (V) although As (III) can also become immobilized in the presence of sulfide (Bissen and Frimmel 2003; Stauder et al. 2005).

However, ML of As from arsenic minerals at neutral pH due to oxidation can occur in heap leach waste (Mend 10.1).

Cyanide leaching is used in 90% of gold ore beneficiation (Yarar 2002). The cyanide used in ore processing degrades into a combination of ammonia, carbonate, and sulfate, wherein ammonia

converts to nitrate ( $\text{NO}_3^-$ ) through the 2-step nitrification process, leaving nitrate as a by-product in the surrounding groundwater and waterways (Akcil 2003). High levels of  $\text{NO}_3^-$  in waterways, and consequently drinking water, can potentially cause methemoglobinemia in infants and gastrointestinal cancer in adults (Kundu et al. 2008). As well, excessive nutrients, such as phosphate and  $\text{NO}_3^-$ , can lead to eutrophication of waterways (Boeykens et al. 2017).

Many methods of removing and/or reducing As and  $\text{NO}_3^-$  from mine waste have been studied. Engineered denitrification systems with woodchips used as a carbon source have been studied and implemented in agricultural settings for the removal of nitrate. These engineered denitrification systems provide an environment that supports the growth of denitrifying bacteria. Denitrifying bacteria utilize nitrate to oxidize woodchip carbon, and in the process reduce  $\text{NO}_3^-$  to  $\text{N}_2$  gas (Blowes et al. 1994; van Driel et al. 2006; Christianson et al. 2010, 2011a,b; Schipper et al. 2010; Woli et al. 2010).

Zero-valent iron (ZVI) has been successfully deployed as a reactive material for the treatment of arsenic (Su and Puls 2001). ZVI immobilizes As by adsorption of As (V) or As (III) onto iron corrosion products in the shell surrounding the elemental iron core and this is sometimes accompanied by reduction As (V) to As (III) (Rao et al. 2009; Manning et al. 2002; Kanel et al. 2006; Bang et al. 2005). Adsorption contributes to the collection of molecules by the internal surface or the external surface of solid matter or by the surface of liquids. Absorption, with which it is often confused, refers to processes in which a substance enters the very interior of crystals, blocks of amorphous solids, or liquids. Adsorption is characterized by the ability of all solid substances to attract molecules of gases or solutions with which they are contacted to their surfaces.

Successful use of ZVI as a reactive material, in conjunction with the development of biological denitrification systems within a permeable reactive barrier (PRB) for the reduction of As and  $\text{NO}_3^-$  have been observed (Lee et al. 2009; Johnson et al. 2008). In spite of successful use of PRBs to treat these contaminants, there is very little data available on the efficacy of PRBs utilizing ZVI and denitrification under cold conditions.

In this bench-scale column experiment, the efficacy of a PRB at low temperature ( $4^\circ\text{C}$ ) was tested. The PRB consisted of ZVI for arsenic adsorption, woodchips for the facilitation of denitrifying bacterial activity to reduce nitrate, and gravel to create an insulating effect. Two columns with varying ratios of woodchips, gravel and ZVI (Tab. 1) were tested. The ratio of amendments and hydraulic residence time (HRT) were adapted from an experiment designed by Lorax Environmental Services Ltd. and implemented by YukonU Research Centre's Industrial Research Chair in Northern Mine Remediation for Newmont Corporation's proposed Coffee Gold Mine.

## **2. Materials and Methods**

### ***2.1. Synthetic Mine Water Preparation***

A synthetic mine water (SMW) stock solution was prepared by adding specific heavy metals into deionized water to reach the concentrations similar to mean concentrations found in mine wastewater analyzed from Golden Predator's Brewery Creek mine located in Yukon. Due to the location's proximity to Coffee Gold mine and similar processing used, Brewery Creek mine was

chosen by Lorax Environmental Services Ltd. as an analog site to model predicted post-closure heap leach waste solution metal concentrations. The SMW stock solution was prepared using the following metal salts:  $\text{KNO}_3$ ,  $\text{MgSO}_4 \cdot 7\text{H}_2\text{O}$ ,  $\text{As}_2\text{O}_5$ , and  $\text{FeCl}_3 \cdot 6\text{H}_2\text{O}$  (Tab. 1). Mass of each metal salt used calculated based on target metal ion concentration (App. A).

Table 1. Metal salts used to reach target concentrations of target metal ions in SMW solution.

<b>Metal Salt</b>	<b>Target Metal Ion</b>	<b>Target Concentration (mg/L)</b>
Potassium Nitrate ( $\text{KNO}_3$ )	Nitrate ( $\text{NO}_3^-$ )	300
Magnesium Sulphate Septahydrate ( $\text{MgSO}_4 \cdot 7\text{H}_2\text{O}$ )	Magnesium (Mg)	200
Arsenic Pentoxide ( $\text{As}_2\text{O}_5$ )	Arsenic ( $\text{As}^{+5}$ )	20
Iron (III) Chloride Hexahydrate ( $\text{FeCl}_3 \cdot 6\text{H}_2\text{O}$ )	Iron (III) ( $\text{Fe}^{+3}$ )	0.5

A total of 16 litres of SMW was prepared for the duration of the experiment based on the calculations of HRT and flow rates (App. B). The SMW was tested for pH, electrical conductivity (EC) and oxidation reduction potential (ORP). pH measurements were performed using a pH meter (650 PCD, Oakton, Vernon, IL, USA) equipped with a double junction Ag/AgCl electrode (Cole Parmer Canada, Montréal, QC, Canada). Calibration of the pH meter was performed before testing using certified buffer solutions (buffer solution pH 10.00; pH 7.00; pH 4.00, Fisher Scientific, Montréal, QC, Canada). Oxidation reduction potential (ORP) measurements were performed using a double junction electrode ORP (ORP Electrode tested. 59001-77, Cole Parmer, Montréal, QC, Canada). Calibration of the ORP meter was performed using a certified solution (ORP Standard, Thermo Fisher Scientific, Waltham, MA, USA). Electrical conductivity (EC) measurements were performed using an EC metre (650 PCD, Oakton, Vernon, IL, USA). Calibration of the EC metre was performed using a certified solution (Conductivity Standard, Thermo Fisher Scientific, Waltham, MA, USA). Two samples were taken of the SMW for metals and nitrate analysis. The metals sample was acidified with  $\text{HNO}_3$

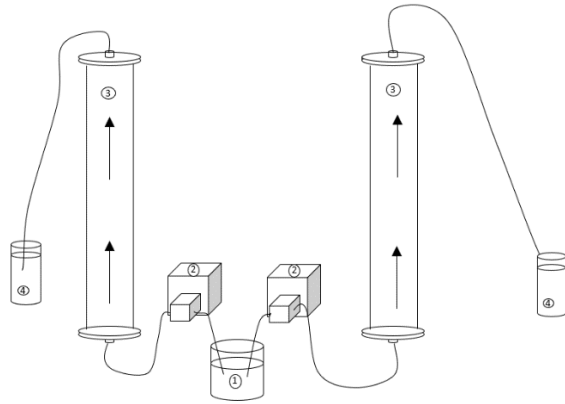


and analyzed via CRC ICPMS by ALS Environmental (Vancouver, BC). The  $\text{NO}_3^-$  sample was acidified with  $\text{H}_2\text{SO}_4$  and analyzed via ion chromatography by ALS Environmental (Vancouver, BC).

## ***2.2. Column Construction***

Two cylindrical columns (Fig. 1) made of 1.1 cm thick Plexiglas™ were used for this experiment. The internal diameter of these columns was 6.4 cm, and the length was 63 cm. Each column was sealed closed at the bottom by bolting a Plexiglas™ plate to it with the same external diameter. Between the column and end plate, a rubber gasket was used to ensure an air-tight seal was achieved. Each end plate was fitted with an outlet port with ~ 1 mm opening hole and sealed additionally with epoxy. L/S Masterflex 16 ID tubing (Cole-Parmer Canada Company, Montreal QC) was attached to the outlet port.

0.45  $\mu\text{m}$  cellulose acetate filter cut to the diameter of the column opening was wetted with deionized water and placed inside of the column against the end plate. To ensure equal distribution of SMW into each column, 139.58 g of Ottawa Sand (Fisher Scientific, Ottawa ON) was placed on top of the filter paper measuring ~ 1 cm in height in each column. The experimental setup was placed in a laboratory refrigerator (Fisher Scientific Isotemp Refrigerator, Ottawa, CA) to ensure a temperature of 4°C was maintained throughout the experiment.



(a)



(b)

Figure 1. (a) Schematic of column design and experimental setup. (1) influent (SMW); (2) peristaltic pump; (3) column; (4) effluent. Schematic is not to scale. (b) Picture of actual experimental setup located in the Yukon U Research Centre Laboratory.

### 2.3 Column Substrates

Each column had a unique mixture of reactive materials. The reactive materials used in this experiment were wood chips, gravel and ZVI. The different percentages of each material were chosen based on a design by Lorax Environmental Services Ltd. (Tab. 2). The ratio was chosen to design a column system which would allow for the treatment outcomes desired through a single-stage system.

The woodchips were sourced from Wiley Mill (Vancouver, BC) and were not representative of available woodland found near the Coffee mine. Gravel was sourced from the City of Whitehorse gravel pit (Whitehorse, YT). The gravel contained limestone and was not

characteristic of the geology found at Coffee Mine. The ZVI was -8 +50 mesh screened and sourced from Connelly GPM (Chicago, IL).

The mass of each substrate was calculated based on the density of each material. Each substrate mixture was amalgamated prior to packing into each column.

Table 2. Substrate (ZVI, gravel and woodchips) ratios of column 1 and column 2.

<b>Substrate</b>	<b>Column 1</b>	<b>Column 2</b>
Woodchips	20%	40%
Gravel	60%	40%
ZVI	20%	20%

#### ***2.4. Hydraulic Residence Time***

A target HRT of 4 days was pre-determined by Lorax Environmental Services Ltd. (Vancouver, BC) in consultation with Dr. David Blowes (University of Waterloo, Waterloo ON). The flow rate was calculated by the pore volume for each column. The pore volume was determined by completely filling each packed column with deionized water (DIW). The volume of DIW used to fill each column was determined to be the pore volume.

#### ***2.5. Experimental Design***

The SMW, Column 1 and 2 were placed in a refrigerator (Fisher Scientific Isotemp Refrigerator, Ottawa, CA) which was maintained at 4 C° for the duration of the experiment (Fig. 1b). SMW was fed via Masterflex peristaltic pumps (Cole-Parmer Canada Company, Montreal QC) from below the columns into the bottom port of each column. The SMW was fed continuously throughout the experiment with the exception of sampling days, wherein flow was stopped temporarily. Volume levels of effluent collected over each 4-day cycle was monitored to ensure target flow rates were maintained. On the 4<sup>th</sup> day of each cycle, flow was stopped, and samples

were taken for nitrate and metals analysis, as well as pH, EC and ORP measurements of the effluent. The effluent was then discarded, and flow was reinitiated into the columns to start the next 4-day cycle.

### **3. Results and Discussion**

#### ***3.1. Porosity and flow rate calculation***

The pore volumes were determined to be 834.9 mL for column 1 and 960.1 mL for column 2. To achieve the target HRT of 4 days the flow rates were back calculated using an HRT of 4 days and the pore volumes using the following formula:

$$\text{Flow rate (m}^3\text{/day)} = \text{pore volume (m}^3\text{)} / \text{HRT (days)} \quad \text{Equation 1}$$

The flow rates were determined to be 0.14 mL/min for column 1 and 0.17 mL/min for column 2 (App. B).

#### ***3.2. Arsenic***

The experiment began with an expected high concentration of As in the SMW influent, at 19.0 mg/L (target As concentration = 20 mg/L (table1)). Once SMW influent passed through each column, dramatic reduction As concentrations decreased dramatically. In column 1, the As concentration decreased to  $6.43 \times 10^{-2}$  mg/L after the initial 12-day period, and in column 2, the As concentration decreased to  $1.12 \times 10^{-3}$  (Fig. 2). Over time, As concentrations continued to trend downward in column 1, eventually reaching a concentration of  $8.10 \times 10^{-4}$  mg/L in effluent collected on the final (28<sup>th</sup>) day of the experiment. In column 2, the As concentration reached its lowest concentration on the 24<sup>th</sup> day at  $9.50 \times 10^{-4}$  mg/L. The As concentration began to rise in

the effluent of column 2 after the 24<sup>th</sup> day, rising from  $9.50 \times 10^{-4}$  mg/L to the final concentration of  $1.81 \times 10^{-2}$  mg/L.

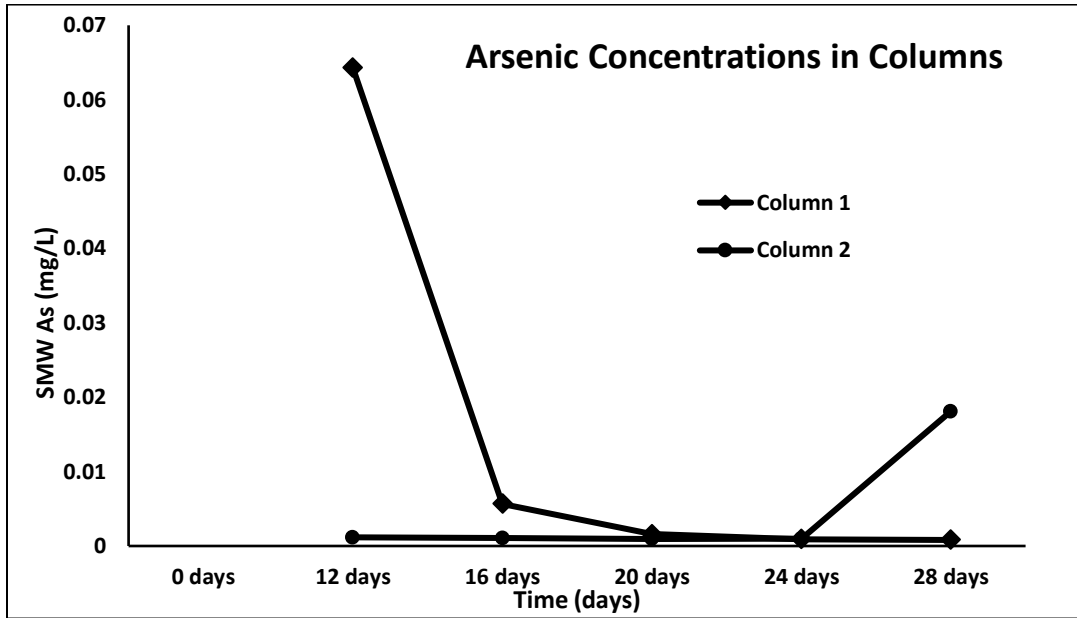


Figure 2. Graph of As concentrations (mg/L) over time throughout the experiment in column 1 and 2.

Overall, there was a high As removal rate of >99.0% observed in both column 1 and column 2 throughout the experiment (Fig. 3). A slight decrease in the removal rate of As in column 2 was observed on the final day, decreasing from 99.99% to 99.92%.

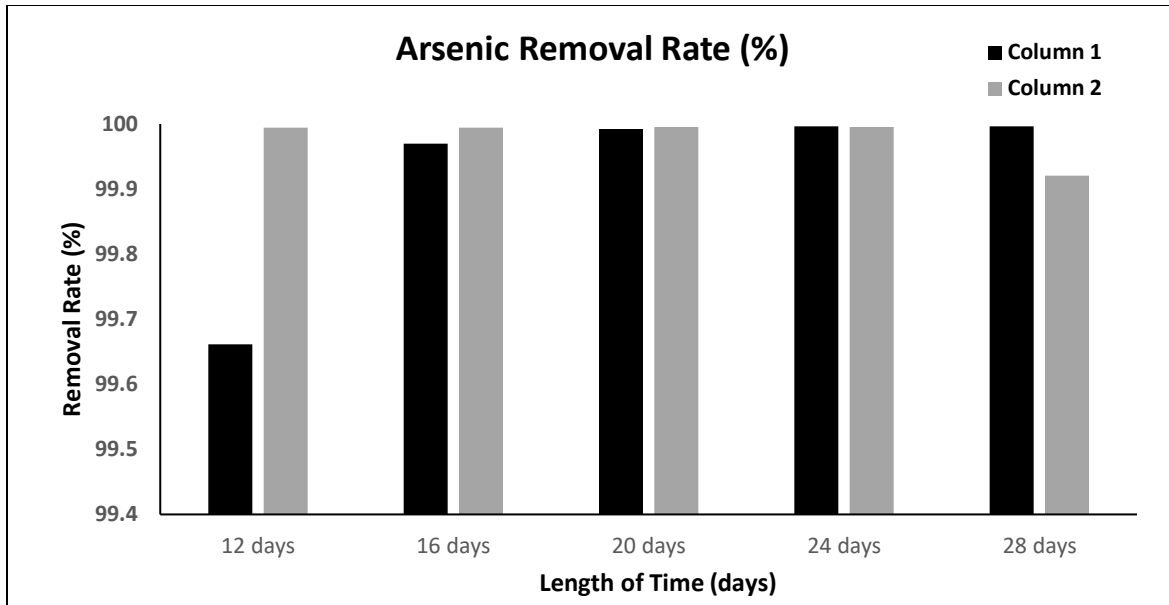


Figure 3. Removal rates (%) of As analyzed in the effluent of column 1 and 2 over time.

The decreased of As concentrations in the SMW throughout the experiment are consistent with the adsorptive qualities of ZVI. Over time, Iron (Fe) concentrations within effluent samples decreased over time in tandem with a decrease in As concentrations (Fig. 4). These findings suggest Fe corrosion products, such as ferrous hydroxide; mixed valence Fe oxides and hydroxides; and ferric oxyhydroxides formed.

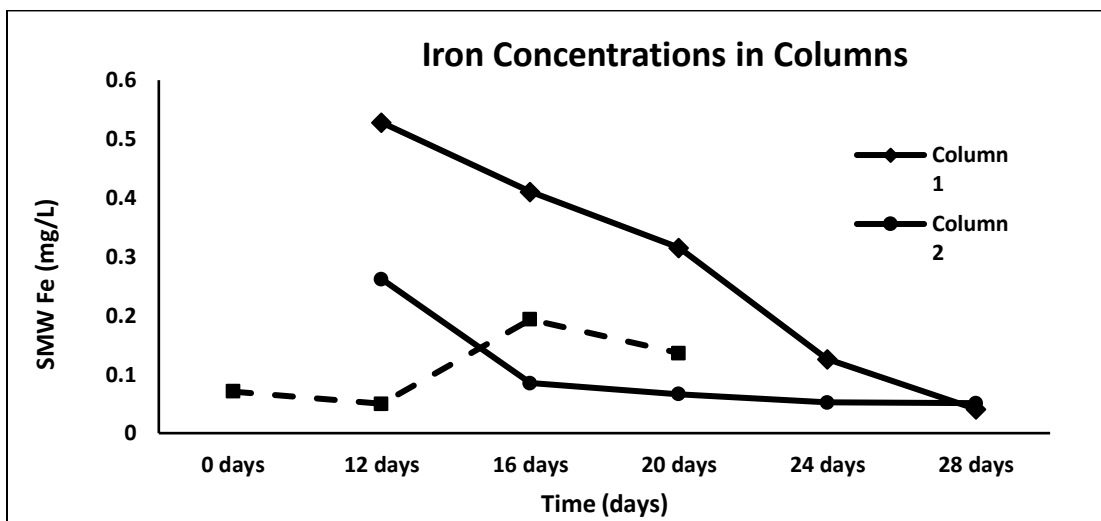


Figure 4. Graph of Fe concentrations over time throughout the experiment of column 1 and 2.

This was further demonstrated by visible greenish deposits, which were likely evidence of iron oxide formation (Fig. 5). Likely, As was adsorbed to ZVI within the columns, and Fe corrosion products complexed with the adsorbed As (Rao et al. 2009).



Figure 5. Green coloured deposit found in columns at end of experiment.

It is unknown whether the As (V) present in the SMW was reduced to As (III) within each of the columns. However, reducing conditions were observed through ORP readings of the effluent from each column throughout the experiment, ranging between -72 mV to -8 mV and -49.5 mV

to -0.3 mV, for Column 1 and 2 respectively. It is possible reduction of As (V) to As (III) occurred.

### ***3.2. Nitrate***

The target  $\text{NO}_3^-$  concentration of the SMW was 300 mg/L, however, upon analysis, the  $\text{NO}_3^-$  concentration was found to be 68.7 mg/L (Fig. 4). To exclude the possibility of faulty measurement of the original metal salt ( $\text{KNO}_3$ ) in the creation of the SMW, back-calculation of the expected concentration of potassium based on the called for weight of  $\text{KNO}_3$ , was found to be 191.26 mg/L. The metals analysis of the SMW showed a potassium concentration of 191.0 mg/L (not shown). It is likely the  $\text{NO}_3^-$  decomposed to various nitrogenous products in solution, such as  $\text{HNO}_3$ ,  $\text{HNO}_2$ ,  $\text{NO}$ ,  $\text{NO}_2$ , etc. (Stern 1972).

Each column produced a reduction of  $\text{NO}_3^-$  of varying concentrations in the first samples of effluent collected. Column 1  $\text{NO}_3^-$  concentration decreased from 68.7 mg/L to 8.43 mg/L and in column 2  $\text{NO}_3^-$  concentration decreased from 68.7 mg/L to 22.4 mg/L at day 12. After day 12,  $\text{NO}_3^-$  concentrations continued to be lower than SMW concentrations, however, removal rates lessened for the rest of the experiment (Fig. 6).



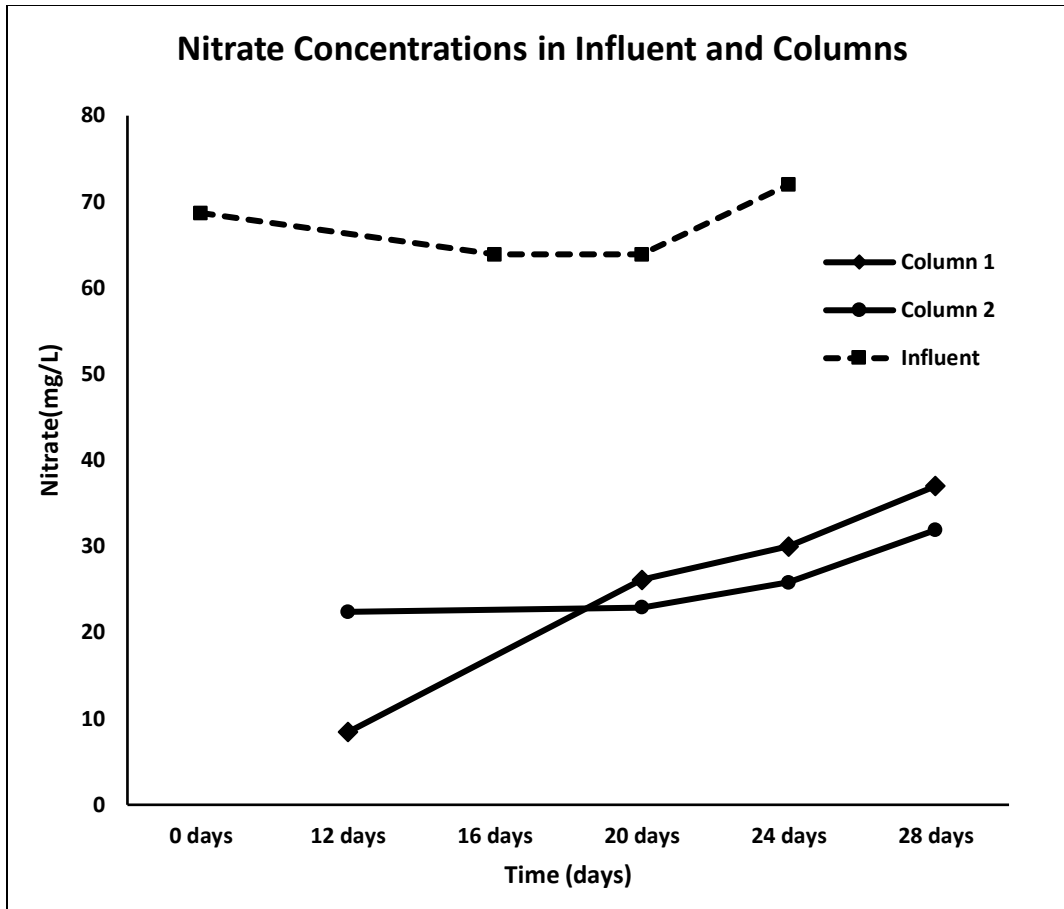


Figure 6. Graph illustrating the concentrations of  $\text{NO}_3^-$  in influent samples and effluent samples of column 1 and 2 over time.

Broadly, removal rates of  $\text{NO}_3^-$  in column 1 decreased from 87.7% to 48.6% over the course of the experiment. Removal rates of  $\text{NO}_3^-$  in column 2 decreased from 67.4% recorded at the beginning of the experiment to 55% removal rate recorded at the end of the experiment.

The concentrations of  $\text{NO}_3^-$  analyzed in the effluent of each column seem to indicate that denitrification is not the mechanism by which  $\text{NO}_3^-$  concentrations decreased in the columns.

Although denitrifying bacteria are known for slow growth in culture (Koike and Hattori 1974), as well as the inhibiting effect cold temperatures can have on growth rates of denitrifying bacteria (Palacin-Lizarbe et al. 2018), the total length of the experiment, 4 weeks, is typically enough time for growth of denitrifying bacteria colonies. If substantial denitrifying bacteria colonies existed, i.e. if the columns were inoculated with bacteria from the gravel and woodchips

amendments, constant  $\text{NO}_3^-$  removal rates throughout the experiment would be observed. In contrast, a declining removal rate in each column was observed (Fig. 7).

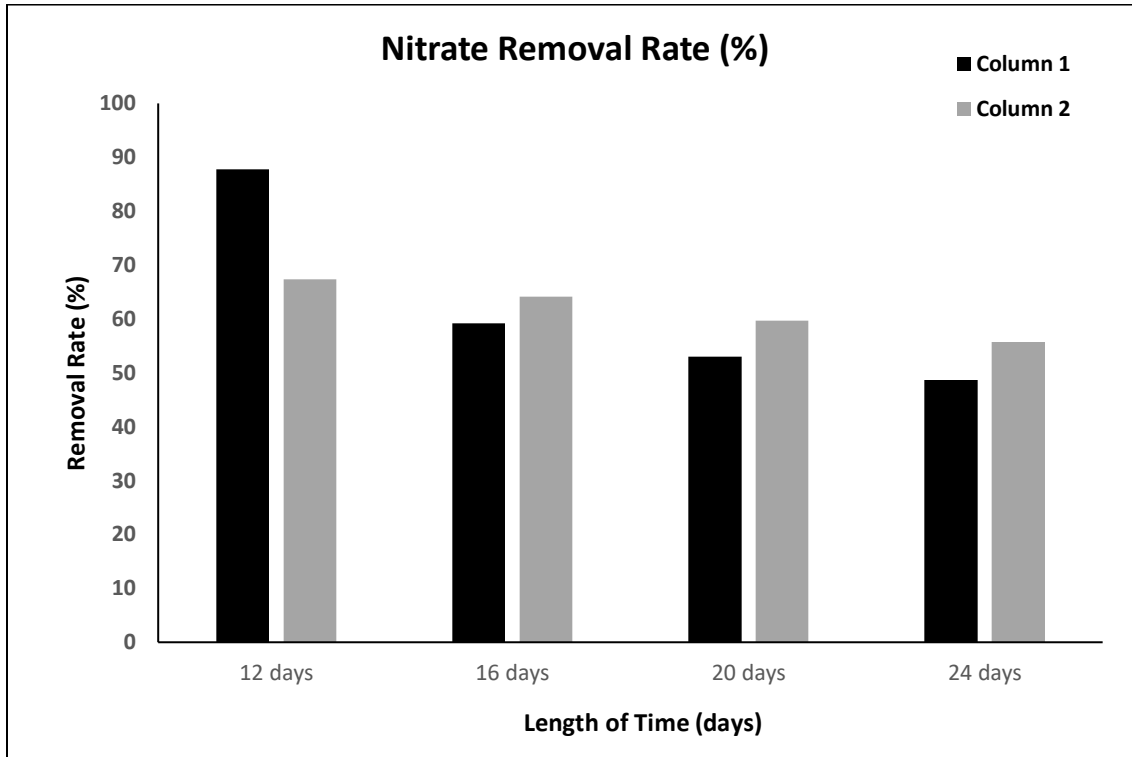


Figure 7. Graph showing  $\text{NO}_3^-$  removal rates in column 1 and 2 over time.

Total organic carbon (TOC) was analyzed in the SMW influent and effluent samples throughout the experiment. TOC analyzed from the effluent samples, had starting concentrations of 205.15 mg/L and 415.58 mg/L, for column 1 and 2 respectively. As no extraneous carbon source was added to the SMW, it is assumed TOC comes from woodchips. This aligns with the ratio percentage of woodchips in each column, as column 1 had 20% woodchips, and column 2 had double, at 40%. Over time, the TOC concentrations in the effluent of each column decreased with rates consistent of natural release of dissolved organic carbon from woodchips in bioreactors (Abusallout and Hua 2017). For this reason, it is unlikely the decrease in carbon over time can be attributed to denitrifying bacteria metabolic processes.

### 3.3. pH

pH analyzed in both the SMW influent, and effluent of each column, showed a progression of very acidic conditions in the SMW influent, pH  $3.80 \pm 0.03$ , to  $8.86 \pm 0.25$  and  $8.06 \pm 1.47$  for columns 1 and 2 respectively (Fig. 8). As the gravel used in the PRB had a makeup that included limestone, it is assumed the dissolution of  $\text{CaCO}_3$  from the limestone created alkaline conditions within the columns, raising the pH overall (Cravotta and Traham 1999).

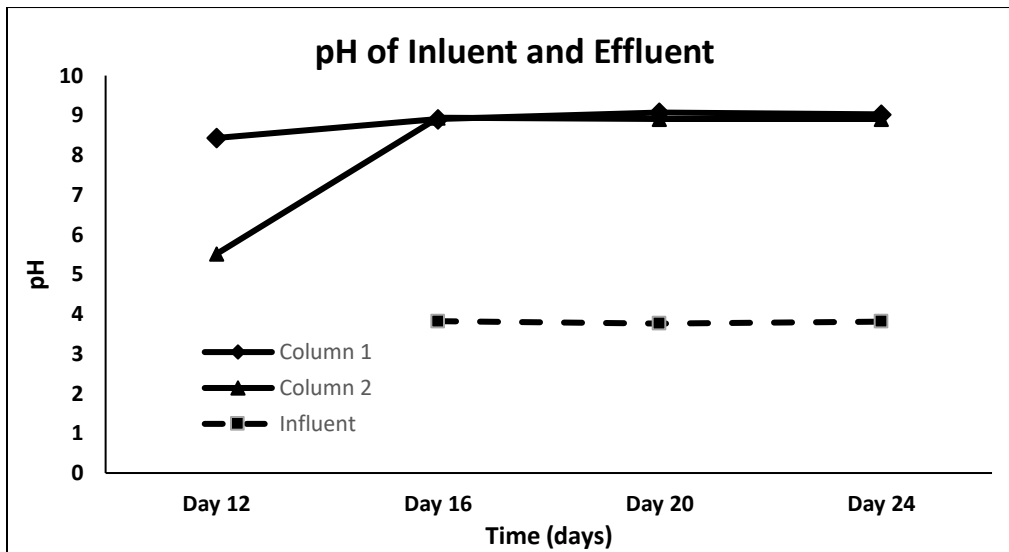


Figure 8. Progression of pH over time in influent and effluent of column 1 and 2.

## 4. Conclusions

Due to possible negative environmental and public health impacts, mitigating excessive metals and nutrient discharge, such as As and  $\text{NO}_3^-$  from heap leach pads is of critical importance to the gold mining industry when considering mine waste management. While mitigation strategies need to be effective, Industry also seeks to reduce costs whenever possible. Bioremediation methods, such as PRBs, may potentially meet these demands. However, there is currently a dearth of research of the use of these methods in cold climates.

The results of this experiment demonstrated, under laboratory conditions, the capability of PRBs in reducing As and  $\text{NO}_3^-$  concentrations to concentrations within the target concentrations for heap leach/passive treatment discharge during closure and water quality objectives (Lorax 2019).

This is especially true for multivalent metals such as the metalloid As, where reactive materials such as ZVI can be used as an adsorbent to remove As under cold climate conditions, as was demonstrated in this experiment.

Although there was a reduction in  $\text{NO}_3^-$  overall, it cannot be determined if this was completed by adsorption or denitrification. Further study is needed to determine the efficacy of reducing  $\text{NO}_3^-$  via denitrification within PRBs in cold climate conditions. Specifically, the use of analyses of parameters such as the progression of  $\text{NO}_2^-$  concentrations, bacteria enumeration assays and genetic identification of existing bacterial colonies within PRBs.

Although there is a large body of literature on the efficacy of PRBs in mining activity, there is still a lack of data on their use in cold climate conditions. Of particular importance, and relevant to the parameters of concern in this experiment, is the ability to cultivate denitrifying bacteria in cold conditions typically found at mine sites in Yukon. Lastly, in light of effects of climate change, varying weather conditions, e.g. high vs low precipitation patterns, should also be considered in future cold climate PRB studies.

## References

- Abusallout I, Hua G. 2017. Characterization of dissolved organic carbon leached from a woodchip bioreactor. *Chemosphere*. 183:36-43.
- Akcil A. 2003. Destruction of cyanide in gold mill effluents: Biological versus chemical treatments. *Biotech Adv*. 21: 501-511.
- Balko BA, Tratnyek PG. 1998. Photoeffects on the reduction of carbon tetrachloride by zero-valent iron. *J Phys Chem*. 102(8): 1459-1465.
- Bang S, Korfiatis GP, Meng X. 2005. Removal of arsenic from water by zero-valent iron. *J Haz Mat*. 121(1-3): 61-67.
- Bissen M, Frimmel FH, 2003. Arsenic-a review. Part 1: occurrence, toxicity, speciation, mobility. *Acta Hydrochim Hydrobiol*. 31(1): 9-18.
- Blowes DW, Jambor JL, Alpers CN. 1994. The environmental geochemistry of sulfide mine-waste. Napan (ON): Mineralogical Association of Canada 438 p.
- Blowes DW, Robertson WD, Ptacek CJ, Merkley C. 1994. Removal of agricultural nitrate from tile-drainage effluent water using in-line bioreactors. *J Contam Hydrol*. 15(3): 207-221.
- Blowes DW, Ptacek CJ, Benner SG, McRae CWT, Bennett TA, Puls RW. 2000. Treatment of inorganic contaminants using permeable reactive barriers. *J Contam Hydrol*. 45(1-2): 123-37.
- Boeykens SP, Piol MN, Legal LS, Saralegui AB, Vazquez C. 2017. Eutrophication decrease: Phosphate adsorption processes in presence of nitrates. *J Env Mgmt*. 203(3): 888-895.
- Cantrell KJ, Kaplan DI, Wietsma TW. 1995. Zero-valent iron for the in-situ remediation of selected metals in groundwater. *J Hazard Mater*. 42(2): 201-12.

- Christianson LE, Bhandari A, Helmers M. 2011a. Pilot-scale evaluation of denitrification drainage bioreactors: Reactor geometry and performance. *J. Env Eng.* 137(4): 213–220.
- Christianson L, Castello A, Christianson R, Helmer M, Bhandari A. 2010. Hydraulic property determination of denitrifying bioreactor fill media. *Appl Eng Agric.* 26(5): 849–854.
- Christianson LE, Hanly JE, Hedley MJ. 2011b. Optimized denitrification bioreactor treatment through simulated drainage containment. *Agric. Water Manage.* 99(1): 85–92
- Cravotta CA, Trahan MK. 1999. Limestone drains to increase pH and remove dissolved metals from acidic mine drainage. *App GeoChem.* 14(5):581-606.
- Diez-Perez I, Sanz F, Gorostiza P. 2006. In situ studies of metal passive films. *Curr Opin Solid State Mat Sci.* 10(3-4): 144-152.
- Farrell J, Kason m, Melitas N, Li T. 2000. Investigation of the long-term performance of zero-valent iron for reductive dichlorination of trichloroethylene. *Env Sci Tech.* 34(3): 514-521.
- Farrell J, Wang J, O’day P, Conklin M. 2001. Electrochemical and spectroscopic study of arsenate removal from water using zero-valent iron media. *Env Sci Tech.* 35(10): 2026-2032.
- Johnson DB. 2003. Chemical and microbiological characteristics of mineral spoils and drainage waters at abandoned coal and metal mines. *Water, Air & Soil Pollut.* 3:47-66.
- Johnson RL, Thoms RB, O’Brien-Johnson R, Nurmi JT, Tratnyek PG. 2008. Mineral precipitation upgradient from a zero-valent iron permeable reactive barrier. *Groundwat Monit & Remed.* 28(3): 56-64.
- Joo SH, Feitz AJ, Waite TD. 2004. Oxidative degradation of the carbothioate herbicide, molinate, using nanoscale zero-valent iron. *Env Sci Tech.* 38(7): 2242-2247.

Kanel SR, Greneche JM, Choi H. 2006. Arsenic (V) removal from groundwater using nano scale zero-valent iron as a colloidal reactive barrier material. *Env Sci Tech.* 40(6): 2045-2050.

Kanel SR, Manning B, Charlet I, Choi H. 2005. Removal of arsenic (III) from groundwater by nanoscale zero-valent iron. *Env Sci Tech.* 39(5): 1291-1298.

Koike I, Hattori A. 1974. Growth yield of a denitrifying bacterium, *Pseudomonas denitricans* under aerobic and denitrifying conditions. *Gen MicroBiol.* 88: 1-10.

Kundu MC, Mandal B, Sarkar D. 2008. Assessment of the potential hazards of nitrate contamination in surface and groundwater in a heavily fertilized and intensively cultivated district of India. *Env Monitor Assess.* 146:183-189.

Lackovic JA, Nikolaidis NP, Dobbs GM. 2000. Inorganic arsenic removal by zero-valent iron. *Env Eng Sci.* 17(1): 29–40.

Lee KJ, Lee Y, Yoon J, Kamala-Kannan S, Park SM, Oh BT. 2009. Assessment of zero-valent iron as a permeable reactive barrier for long-term removal of arsenic compounds from synthetic water. *Env Tech.* 30(13): 1425-1434.

Li XQ, Elliott DW, Zhang WX. 2006. Zero-valent iron nanoparticles for abatement of environmental pollutants: material and engineering aspects. *Crit Rev in Solid State & Mat Sci.* 31(4): 111-122.

Martin A, Nieuwenberg J, Flather D. 2019. Coffee Gold Project: Work plan to demonstrate feasibility of passive bioremediation treatment of heap leach rinse solutions at closure. Technical Memorandum.

Manning BA, Hunt ML, Amrhein C, Yarmoff JA. 2002. Arsenic (III) and Arsenic (V) reactions with zerovalent iron corrosion products. *Env Sci Tec.* 36(24): 5455-5461.

Morrison SJ, Metzler DR, Carpenter CE. 2001. Uranium precipitation in a permeable reactive barrier by progressive irreversible dissolution of zerovalent iron. *Env Sci Tech.* 35(2): 385–90.

Noubactep C. 2008. A critical review on the process of contaminant removal in  $\text{Fe}^0 - \text{H}_2\text{O}$  systems. *Env Tech.* 29(8): 909-920.

Palacin-Lizarbe C, Camarero L, Catalan J. 2018. Denitrification temperature dependence in remote, cold and N-poor lake sediments. *Wat Resour Res.* 54(2): 1161-1173.

Puls RW, Paul CJ, Powell RM. 1999. The application of in situ permeable reactive (zero-valent iron) barrier technology for the remediation of chromate-contaminated groundwater: a field test. *Appl Geochem.* 14(8): 989–1000

Rao P, Mak MSH, Liu T, Lai KCK, Lo IMC. 2009. Effects of humic acid on arsenic (V) removal by zero-valent iron from groundwater with special references to corrosion products analyses. *Chemosphere.* 75(2): 156-162.

Reinsch BC, Forsberg B, Penn RL, Kim CS, Lowry GV. 2010. Chemical transformations during aging of zerovalent iron nanoparticles in the presence of common groundwater dissolved constituents. *Env Sci Tech.* 44(9): 3455-3461.

Roussel C, Neel C, Bril H. 2000. Minerals controlling arsenic and lead solubility in an abandoned gold mine tailings. *Sci Total Env.* 263: 209-219.

Schipper LA, Robertson WD, Gold AJ, Jaynes DB, Cameron SC. 2010. Denitrifying bioreactors: An approach for reducing nitrate loads to receiving waters. *Ecol Eng.* 36(11): 1532–1543.



Shokes TE, Moller G. 1999. Removal of dissolved heavy metals from acid rock drainage using iron metal. *Environ Sci Tech.* 33( :282–7.

Stauder S, Raue B, Sacher F. 2005. Thioarsenates in sulfidic waters. *Env Sci Tech.* 39(16): 5933-5939.

Stern K. 1972. High temperature properties and decomposition of inorganic salts part 3, nitrates and nitrites. *Phys & Chem Ref Data.* 1(3): 747-771.

Su C, Puls RW. 2001. Arsenate and arsenite removal by zerovalent iron: kinetics redox transformation and implications for in situ groundwater remediation. *Env Sci Tech.* 35(7): 1487-1492.

van Driel PW, Robertson WD, Merkley IC. 2006. Upflow reactors for riparian zone denitrification. *J Env Qual.* 35(2): 412-420.

Woli KP, David MB, Cooke RA, McIsaac GR, Mitchell CA. 2010. Nitrogen balance in and export in and export from agricultural fields associated with controlled drainage systems and denitrifying bioreactors. *Ecol Eng.* 36(11): 1558–1566

Yarar B. 2002. Long term persistence of cyanide species in mine waste environments. *Tailing & Mine Waste. Tailings and Mine Waste 2002*

## Appendix A

### Calculation of Target Metal Ion Concentrations in SMW

#### Arsenic

Metal salt used:  $\text{As}_2\text{O}_5$ , 229.8402 g/mol

Target metal ion concentration: 20.0 mg/L\*

#### % Ratio

$$\text{As} = 149.8 \text{ g/mol} / 229.8402 \text{ g/mol} = 65.18\%$$

$$20 \text{ mg} = 0.02 \text{ g}$$

$$\frac{0.02 \text{ g}}{x \text{ g}} \times \frac{65.18\%}{100\%}$$

$$x = 0.0307 \text{ g/L of } \text{As}_2\text{O}_5$$

#### Nitrate

Metal salt used:  $\text{KNO}_3$ , 101.1032 g/mol

Target metal ion concentration: 300.0 mg/L

#### % Ratio

$$\text{NO}_3 = 62.006 \text{ g/mol} / 101.1032 \text{ g/mol} = 61.33\%$$

$$300 \text{ mg} = 0.30 \text{ g}$$

$$\frac{0.30 \text{ g}}{x \text{ g}} \times \frac{61.33\%}{100\%}$$

$$x = 0.4892 \text{ g/L of } \text{KNO}_3$$

#### Magnesium

Metal salt used:  $\text{MgSO}_4 \cdot 7\text{H}_2\text{O}$ , 246.48 g/mol

Target metal ion concentration: 200.0 mg/L

#### % Ratio

$$\text{Mg} = 24.3 \text{ g/mol} / 246.48 \text{ g/mol} = 9.86\%$$

$$200 \text{ mg} = 0.20 \text{ g}$$

$$\frac{0.20 \text{ g}}{x \text{ g}} \times \frac{9.86\%}{100\%}$$

$$x = 2.03 \text{ g/L of } \text{MgSO}_4 \cdot 7\text{H}_2\text{O}$$

## Iron

Metal salt used:  $\text{FeCl}_3 \cdot 7\text{H}_2\text{O}$ , 270.30 g/mol

Target metal ion concentration: 0.5 mg/L

% Ratio

$$\text{Fe} = 55.8 \text{ g/mol} / 270.30 \text{ g/mol} = 20.64\%$$

$$0.5 \text{ mg} = 0.0005 \text{ g}$$

$$\frac{0.0005 \text{ g}}{x \text{ g}} \times \frac{20.64\%}{100 \%}$$

$$x = 0.0024 \text{ g/L of } \text{FeCl}_3 \cdot 7\text{H}_2\text{O}$$

\*20 mg/L was used as the target concentration for arsenic due to a misreading of projected heap leach solution arsenic concentrations for Coffee Gold mine. The actual projected concentration is 2.0 mg/L of arsenic.

## Appendix B

### Calculation of Flow Rates in Column 1 and 2

Equation: Flow rate ( $\text{m}^3/\text{day}$ ) = pore volume ( $\text{m}^3$ ) / HRT (days)

#### Column 1

Pore volume = 834.9 mL or  $8.35 \times 10^{-4} \text{ m}^3$

HRT target = 4 days

Flow rate ( $\text{m}^3/\text{day}$ ) =  $8.35 \times 10^{-4} \text{ m}^3 / 4 \text{ days}$

Flow rate =  $2.087 \times 10^{-4} \text{ m}^3 / \text{day}$

Flow Rate = 208.73 mL / day

Flow Rate = 0.14 mL/min

#### Column 2

Pore volume = 960.1 mL or  $9.60 \times 10^{-4} \text{ m}^3$

HRT target = 4 days

Flow rate ( $\text{m}^3/\text{day}$ ) =  $9.60 \times 10^{-4} \text{ m}^3 / 4 \text{ days}$

Flow rate =  $2.40 \times 10^{-4} \text{ m}^3 / \text{day}$

Flow Rate = 240.025 mL / day

Flow Rate = 0.17 mL/min